

Flooding Regularization for Stable Training of Generative Adversarial Networks

Iu Yahiro¹

yahiro@ms.k.u-tokyo.ac.jp

Takashi Ishida^{2,1}

ishi@k.u-tokyo.ac.jp

Naoto Yokoya^{1,2}

yokoya@k.u-tokyo.ac.jp

¹The University of Tokyo ²RIKEN

Abstract

Generative Adversarial Networks (GANs) have shown remarkable performance in image generation. However, GAN training suffers from the problem of instability. One of the main approaches to address this problem is to modify the loss function, often using regularization terms in addition to changing the type of adversarial losses. This paper focuses on directly regularizing the adversarial loss function. We propose a method that applies flooding, an overfitting suppression method in supervised learning, to GANs to directly prevent the discriminator’s loss from becoming excessively low. Flooding requires tuning the flood level, but when applied to GANs, we propose that the appropriate range of flood level settings is determined by the adversarial loss function, supported by theoretical analysis of GANs using the binary cross entropy loss. We experimentally verify that flooding stabilizes GAN training and can be combined with other stabilization techniques. We also reveal that by restricting the discriminator’s loss to be no greater than flood level, the training proceeds stably even when the flood level is somewhat high.

1. Introduction

Generative Adversarial Networks (GANs) [7] are one of the learning frameworks for generative models proposed by Goodfellow et al., and they have shown remarkable performance in a wide range of image generation tasks [5, 17, 23, 35]. GANs are based on a learning strategy where two models, a generator G and a discriminator D , compete against each other. The generator takes a noise vector z sampled from a known distribution \mathbb{P}_z (primarily the standard normal distribution) as input and produces a generated image $G(z)$ as output. The discriminator D takes either real images sampled from the target underlying distribution \mathbb{P}_r , or generated images as input \mathbf{x} and outputs $D(\mathbf{x})$. The discriminator is designed to correctly distinguish between real and generated images, while the generator aims to reduce the discriminator’s performance on generated images. By designing the loss function in this way, the distribution

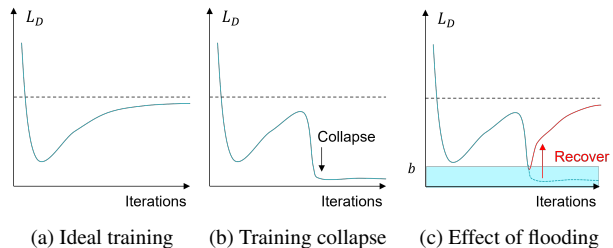


Figure 1. Overview of the discriminator loss (L_D) progress in GANs and the effect of flooding. In ideal training (a), the discriminator loss rises steadily to loss at the convergence (dotted line), and the training will converge. On the other hand, when the training collapses (b), the discriminator loss falls sharply from a certain point and will stay at a very low value. By applying flooding with flood level b , we can suppress the rapid decline in the discriminator’s loss, thereby stabilizing the training.

of generated images \mathbb{P}_g becomes similar to that of real images. Goodfellow et al. defined this adversarial structure using the following min-max formulation of the value function V , involving the generator G and the discriminator D .

$$\min_G \max_D V(D, G) = \mathbb{E}_{\mathbf{x} \sim \mathbb{P}_r} [\log(D(\mathbf{x}))] + \mathbb{E}_{z \sim \mathbb{P}_z} [\log(1 - D(G(z)))]. \quad (1)$$

Although GANs successfully tackle the task of generating images according to this strategy, instability in training persists as a problem. Some research [1, 26] pointed out that the training is likely unstable since the discriminator is often unstable, and the discriminator’s loss becomes excessively low. In the training, the generator updates according to its loss based on the performance of the discriminator on identifying real or generated images. However, if the performance is too high, the generator will lose the proper gradient, and the training and generated images will collapse.

Previous research has proposed methods to improve the instability issue. These are mainly categorized as changes in adversarial losses, regularization, and architectural changes [31]. The adversarial loss is the loss that creates an adversarial structure between the generator and discriminator. For example, GANs proposed by Goodfellow et al. use the binary cross entropy loss (BCE loss) as the adversar-

ial loss based on formula 1. However, previous research [2, 19, 20] showed that BCE loss causes instability and proposes changes to stabilize the training.

On the other hand, some research adds regularization to GAN training, and one main approach is to add a regularization term to the adversarial loss that leads to training stabilization. It can be combined with changes in adversarial losses without changing the theoretical convergence ($\mathbb{P}_g = \mathbb{P}_r$) and does not need to be balanced by a coefficient, as the addition of a regularization term. For example, gradient penalty used in WGAN-GP [8] is a regularization term that encourages the gradient norm to be closer to 1, which prevents gradient explosion and vanishing. The loss functions of the discriminator and generator can be generalized with the changes in the type of adversarial losses and the addition of regularization terms and can be expressed as

$$\begin{aligned} L_D &= L_{D,\text{adv}} + \sum_i \lambda_{D,i} L_{D,\text{aux},i}, \\ L_G &= L_{G,\text{adv}} + \sum_i \lambda_{G,i} L_{G,\text{aux},i}, \end{aligned} \quad (2)$$

where $L_{D,\text{adv}}$ and $L_{G,\text{adv}}$ are the adversarial losses for the discriminator and generator, respectively, and $L_{D,\text{aux},i}$ and $L_{G,\text{aux},i}$ are the i th regularization terms. Also, $\lambda_{D,i}$ and $\lambda_{G,i}$ are coefficients representing the weight of the i th regularization terms. The adversarial losses are calculated using the discriminator outputs for real or generated images as

$$\begin{aligned} L_{D,\text{adv}} &= L_{D,\text{real}} + L_{D,\text{fake}} \\ &= \mathbb{E}_{\mathbf{x} \sim \mathbb{P}_r} [f_{D,\text{real}}(\mathbf{x})] + \mathbb{E}_{\mathbf{x} \sim \mathbb{P}_g} [f_{D,\text{fake}}(\mathbf{x})], \\ L_{G,\text{adv}} &= \mathbb{E}_{\mathbf{x} \sim \mathbb{P}_g} [f_G(\mathbf{x})], \end{aligned} \quad (3)$$

where $L_{D,\text{real}}$ and $L_{D,\text{fake}}$ are the discriminator’s losses for real and generated images, respectively, and $f_{D,\text{real}}$, $f_{D,\text{fake}}$, and f_G are functions that take the discriminator’s output as input and output the loss. Some studies further improved the stability by combining changes in the type of adversarial losses with the addition of regularization terms. For example, WGAN-GP improves performance by adding gradient penalty as a regularization term while changing the adversarial loss type to Wasserstein loss [8]. However, adding a regularization term requires tuning $\lambda_{D,\text{aux},i}$ and $\lambda_{G,\text{aux},i}$. Other regularization techniques include spectral normalization [22] and weight clipping in WGAN [2], which normalizes the weights of the model, and label smoothing [26], which involves modifying the target labels.

This paper proposes a direct regularization technique for the adversarial loss function, which stabilizes GAN training by applying regularization to adversarial loss values while preserving the nature of the adversarial loss. We explore a new technique that directly prevents the phenomenon in which the discriminator’s loss becomes excessively low. This phenomenon can be regarded as a state in which the discriminator overfits discriminating between generated and

real images. Therefore, we propose the application of *flooding* [11], a method for preventing overfitting in supervised image classification, to GANs. In order to prevent an excessive decrease in loss L when the prediction model overfits, flooding recalculates loss h given by

$$h(L, b) = |L - b| + b. \quad (4)$$

Here, b is called the flood level. Due to the absolute operator, the gradient will be flipped when the loss becomes smaller than b , preventing the model from overfitting. Note that the adding back b of Eq. (4) does not affect the gradient, Ishida et al. adopted the definition to ensure that $h(L, b) = L$ where $L \geq b$. The flood level is a hyperparameter that requires tuning.

Our contributions are as follows.

1. We propose applying flooding, preventing overfitting in supervised learning, to the GAN training. It stabilizes the training as shown in Figure 1.
2. We introduce a novel approach to set the flood level based on theoretical loss values obtained during training convergence across various adversarial losses.
3. We demonstrate that flooding stabilizes the GAN training experimentally. We also show that flooding is effective when the flood level is not too low and combined with existing stabilization methods, such as changes in adversarial loss type and architecture.

2. Related Work

In this section, we first review stabilization methods for training GANs, change of adversarial loss type, regularization, and change of architectures. Next, we show application of adversarial architectures and methods for overfitting in supervised learning.

2.1. Stabilization methods for training GANs

There are three categories in stabilization methods for the GAN training: change of adversarial loss type, regularization, and change of architectures [31].

Change of adversarial loss type Table 1 summarizes six examples of adversarial loss functions. Goodfellow et al. [7] pointed out that the original loss function given in Eq. (1) can lead to a problem that the discriminator can correctly discriminate most of the generated images ($D(G(\mathbf{z})) \simeq 0$), resulting in saturated gradients of the generator. To solve it, Goodfellow et al. modified f_G to the non-saturating BCE loss shown in Table 1.

However, even with the modification, the instability remains [1, 26]. Goodfellow et al. have shown that the training with BCE loss minimizes the Kullback–Leibler (KL) divergence between the distribution of the generated and real images. Arjovsky et al. [2] showed that the minimization of KL divergence causes instability, and they proposed

Adversarial loss	$f_{D,\text{real}}$	$f_{D,\text{fake}}$	f_G
BCE loss [7]	$-\log(D(\mathbf{x}))$	$-\log(1 - D(G(\mathbf{z})))$	$\log(1 - D(G(\mathbf{z})))$
BCE loss (non-saturating) [7]	$-\log(D(\mathbf{x}))$	$-\log(1 - D(G(\mathbf{z})))$	$-\log(D(G(\mathbf{z})))$
Wasserstein loss [2]	$-D(\mathbf{x})$	$D(\mathbf{x})$	$-D(G(\mathbf{z}))$
Hinge loss [19]	$\max(0, 1 - D(\mathbf{x}))$	$\max(0, 1 + D(G(\mathbf{z})))$	$-D(G(\mathbf{z}))$
Least squares loss [20]	$\frac{1}{2}(D(\mathbf{x}) - b_{\text{LS}})^2$	$\frac{1}{2}(D(G(\mathbf{z})) - a_{\text{LS}})^2$	$\frac{1}{2}(D(G(\mathbf{z})) - c_{\text{LS}})^2$
BCE loss (smoothing) [26]	$\text{BCE}_{\text{sm}}(D(\mathbf{x}), b)$	$\text{BCE}_{\text{sm}}(D(G(\mathbf{z})), a)$	$-\log(D(G(\mathbf{z})))$

Table 1. Examples of adversarial loss functions. One of the setting a_{LS} , b_{LS} , and c_{LS} proposed by Mao et al. [20] is (0, 1, 1). Furthermore, a and b denote labels for real and generated images, respectively; for example, a, b is set to (0.9, 0.0) in one-sided label smoothing [26]. $\text{BCE}_{\text{sm}}(x, y) = -y \cdot \log(x) - (1 - y) \cdot \log(1 - x)$ is defined to shorten the expression.

Adversarial loss	$L_{D_{\text{opt}},\text{real}}$	$L_{D_{\text{opt}},\text{fake}}$	$L_{D_{\text{opt}}}$	$L_{G_{\text{opt}}}$	Flooding type
BCE loss [7]	$\log 2$	$\log 2$	-	$-\log 2$	1,2,3
BCE loss (non-saturating) [7]	$\log 2$	$\log 2$	-	$\log 2$	1,2,3
Wasserstein loss [2]	-	-	0	-	3
Hinge loss [19]	-	-	2	1	3
Least squares loss [20]	$\frac{(a_{\text{LS}} - b_{\text{LS}})^2}{8}$	$\frac{(a_{\text{LS}} - b_{\text{LS}})^2}{8}$	-	$\frac{(a_{\text{LS}} + b_{\text{LS}} - 2c_{\text{LS}})^2}{8}$	1,2,3
BCE loss (smoothing) [26]	$\text{BCE}_{\text{sm}}(\frac{a+b}{2}, b)$	$\text{BCE}_{\text{sm}}(\frac{a+b}{2}, a)$	-	$-\log(\frac{a+b}{2})$	1,2,3

Table 2. The theoretical loss values for each adversarial loss when the training reaches the convergence. If $L_{D_{\text{opt}},\text{real}}$ and $L_{D_{\text{opt}},\text{fake}}$ cannot be determined as a real number, only $L_{D_{\text{opt}}}$ is shown, and if those can be determined, the apparent $L_{D_{\text{opt}}}$ ($= L_{D_{\text{opt}},\text{real}} + L_{D_{\text{opt}},\text{fake}}$) is omitted. Also, omit the Wasserstein loss $L_{G_{\text{opt}}}$ since it is not uniquely determined.

Wasserstein loss based on Earth Mover (EM) distance (Table 1). Lim et al. [19] proposed Geometric GAN using a hinge loss, and Mao et al. [20] proposed Least Squares GANs (LSGAN) based on minimizing Pearson χ^2 distance. Table 1 shows the losses as hinge loss and LSGAN loss. These methods can be regarded as integral probability metric (IPM)-based regularization [31], where the generators and discriminators belong to a particular function class, such as models with Lipschitz continuity.

It is crucial to mathematically prove that the distribution \mathbb{P}_g of the generated images at training convergence matches the distribution \mathbb{P}_r of the dataset when changing the adversarial loss functions [7, 19, 20]. Note that the proof requires the assumption that infinite data from \mathbb{P}_r and ideal models are available for the training. Therefore, it cannot be perfectly reproduced in experiments, but it is useful to make theoretical analysis easy and acquire insightful knowledge. Some research follows proof procedure described below.

1. Find a discriminator D^* , which minimizes the loss for a fixed generator G .
2. Find a generator G_{opt} , which minimizes D^* loss.

Let $L_{D^*} = L_{D^*,\text{real}} + L_{D^*,\text{fake}}$ denote the loss of D^* , $L_{D_{\text{opt}}}$ denote the loss of the discriminator in step 2 (D_{opt}), and $L_{G_{\text{opt}}}$ denote the loss of the generator in step 2. Table 2 shows $L_{D_{\text{opt}},\text{real}}$, $L_{D_{\text{opt}},\text{fake}}$, $L_{D_{\text{opt}}}$, and $L_{G_{\text{opt}}}$ for each adversarial loss.

Regularization There are various regularization techniques to stabilize the GAN training, and one major approach is to

add a regularization term to the loss function. The training is based on the competition defined by the adversarial loss, and some auxiliary loss terms other than the adversarial loss increase the stability. These methods directly prevent gradient explosion and vanishing [16, 24], model overfitting [2, 3], and mode collapse [4]. Gradient penalty [8] is an example of adding a regularization term, which improves the discriminator stability by adding a squared error between the gradient norm and 1 to the adversarial loss so that the gradient norm approaches 1. It has been applied to WGAN-GP [8] and contributes to training stabilization. These methods require tuning of the coefficients to balance the adversarial loss. Label smoothing [26] regularizes through the target labels and stabilizes the training that modifies non-saturating BCE loss as in Table 1. However, it is primarily used with BCE loss, and its stabilization effect is not known for other adversarial losses. Normalization is another common approach to regularization [22, 32]. Spectral normalization [22], a representative normalization technique for GANs, stabilizes training by controlling the Lipschitz constant of the discriminator through the normalization of weight matrices. Unlike the existing regularization techniques for GANs, our method directly regularizes the adversarial loss.

Change of architecture Changing the architecture is a commonly used approach to stabilizing GAN training. For example, when generating images with a high resolution, a method that efficiently preserves the features of the entire image is essential. Deep convolutional GAN (DC-

GAN) [25], which employs a convolutional layer, and Self-Attention GAN (SAGAN) [33], which introduces an attention mechanism, have been proposed. Some studies [3, 13–15] have proposed to generate high-resolution and photorealistic images by devising architectures. These model changes are relatively easy to combine with loss changes because they do not disrupt the competing structure of GANs, which is represented by adversarial losses.

2.2. Various application of adversarial architectures

Goodfellow et al. [7] proposed GANs as a method for image generation tasks with unlabeled data. On the other hand, GAN techniques have emerged that utilize the advantage that adversarial architectures perform well in training a generator of high-dimensional distributions. For instance, Mirza et al. [21] proposed conditional GANs to control generated images with labels. They were designed to feed labels both of the generator and the discriminator, and the idea was employed for a wide range of applications, such as text-to-image generation [34] and image-to-image translation [12]. Additionally, domain-adversarial neural network (DANN) [6] and adversarial discriminative domain adaptation (ADDA) [30] proposed the use of adversarial frameworks for domain adaptation, which alleviates the gap between the training (source) and the test (target) domain in discriminative tasks. These adversarial architectures also have challenges with how to train multiple models.

2.3. Methods for overfitting in supervised learning

In supervised learning, overfitting is a well-known phenomenon in which a model achieves good accuracy only for training data and cannot predict well for unknown data. Typical methods for preventing overfitting of deep models in supervised learning are dropout [28], batch normalization [10], data augmentation [27], and label smoothing [29]. Many of these techniques can be applied not only to supervised learning but also to other domains, and they are sometimes adopted in GANs as well [18]. Ishida et al. [11] proposed flooding, a method that recalculates the loss based on the formula 4 with respect to the flood level b so that the loss does not become extremely small and avoids overfitting. While this method performs well in supervised learning, there is no standard for setting b to avoid extremely low losses, and it requires a tuning process through experiments.

3. Method

In this section, we first provide an overview of GAN training, and propose the application of flooding to GANs. In the proposal, we show that there are several ways to apply flooding to GANs and discuss the flood level setting.

3.1. Overview of GAN training

GAN training has a generator G and a discriminator D and proceeds based on losses defined in Eq. (2). This section assumes simple GANs without any regularization term to simplify the discussion. The losses are expressed as

$$L_D = L_{D,adv}, L_G = L_{G,adv}. \quad (5)$$

For example, for GANs with BCE losses [7], L_G and L_D can be written as

$$\begin{aligned} L_D &= \mathbb{E}_{\mathbf{x} \sim \mathbb{P}_r} [-\log(D(\mathbf{x}))] + \mathbb{E}_{\mathbf{x} \sim \mathbb{P}_g} [-\log(1 - D(\mathbf{x}))], \\ L_G &= \mathbb{E}_{\mathbf{x} \sim \mathbb{P}_g} [\log(1 - D(\mathbf{x}))]. \end{aligned} \quad (6)$$

3.2. Application of flooding to GANs

One of the causes of instability in GANs is the case where the discriminator’s loss becomes excessively low, which can be regarded as an overfitting of the discriminator in the task of discriminating between generated and real images. Flooding is a method for preventing overfitting in supervised learning. We aim to improve the stability of GAN training by applying flooding to the discriminator. In this case, we need to consider “how to apply flooding to GANs” and “how to set the flood level,” which are explained in the following sections.

3.2.1 How to apply flooding to GANs

Flooding is applied to Eq. (5) to avoid the overfitting of the discriminator. There are three ways to apply flooding to the discriminator, depending on the inserting position of the operation h defined in Eq. (4),

$$\begin{aligned} L_{D,\text{flood},1} &= \mathbb{E}_{\mathbf{x} \sim \mathbb{P}_r} [h(f_{D,\text{real}}(D(\mathbf{x})), b_{\text{real}})] \\ &\quad + \mathbb{E}_{\mathbf{x} \sim \mathbb{P}_g} [h(f_{D,\text{fake}}(D(\mathbf{x})), b_{\text{fake}})], \\ L_{D,\text{flood},2} &= h(\mathbb{E}_{\mathbf{x} \sim \mathbb{P}_r} [f_{D,\text{real}}(D(\mathbf{x}))], b_{\text{real}}) \\ &\quad + h(\mathbb{E}_{\mathbf{x} \sim \mathbb{P}_g} [f_{D,\text{fake}}(D(\mathbf{x}))], b_{\text{fake}}), \\ L_{D,\text{flood},3} &= h(\mathbb{E}_{\mathbf{x} \sim \mathbb{P}_r} [f_{D,\text{real}}(D(\mathbf{x}))] \\ &\quad + \mathbb{E}_{\mathbf{x} \sim \mathbb{P}_g} [f_{D,\text{fake}}(D(\mathbf{x}))], b_{\text{all}}), \end{aligned} \quad (7)$$

where b_{real} and b_{fake} are the flood levels for adversarial losses for real and generated images, respectively, and b_{all} is the flood level for overall adversarial losses. The appropriate setting of these flood levels and suitable loss functions for the three types are discussed in the next section.

3.2.2 How to set the flood level

The appropriate setting of the flood level b_{real} , b_{fake} , and b_{all} is important. In supervised learning, because the loss at convergence is not uniquely determined because it depends on models and datasets, the flood level is a hyperparameter, and the appropriate range of its setting that does not depend on datasets and other factors has not yet been shown.

$L_{D_{\text{opt}},\text{real}}$, $L_{D_{\text{opt}},\text{fake}}$, or their sum $L_{D_{\text{opt}}}$ is uniquely determined, as summarized in Table 2, and we propose the following hypotheses about the setting of the flood level.

Hypothesis 1. *If $L_{D_{\text{opt}},\text{real}}$ and $L_{D_{\text{opt}},\text{fake}}$ are uniquely determined, then b_{real} and b_{fake} should be set to satisfy the following condition (8), either $L_{D,\text{flood},1}$ or $L_{D,\text{flood},2}$ can stabilize the training. The training will collapse if the condition (8) is unsatisfied.*

$$(b_{\text{real}} < L_{D_{\text{opt}},\text{real}}) \wedge (b_{\text{fake}} < L_{D_{\text{opt}},\text{fake}}) \quad (8)$$

Hypothesis 2. *If $L_{D_{\text{opt}}}$ is uniquely determined, then b_{all} should be set to satisfy the following condition (9), and $L_{D,\text{flood},3}$ can stabilize the training. The training will collapse if the condition (9) is unsatisfied.*

$$b_{\text{all}} < L_{D_{\text{opt}}} \quad (9)$$

When there is a possibility of excessively low loss for each of uniquely determined $L_{D_{\text{opt}},\text{real}}$ and $L_{D_{\text{opt}},\text{fake}}$, we suppose to apply $L_{D,\text{flood},1}$ and $L_{D,\text{flood},2}$ among the three types shown in Eq. (7). This is the inspiration for Hypothesis 1. For example, since $L_{D_{\text{opt}},\text{real}}$ and $L_{D_{\text{opt}},\text{fake}}$ are $\log 2$ for GANs with BCE loss, b_{real} and b_{fake} should be set within the range $0 \leq D(\mathbf{x}) \leq 1$ and lower than $\log 2$. On the other hand, there are cases where $L_{D_{\text{opt}},\text{real}}$ and $L_{D_{\text{opt}},\text{fake}}$ are not uniquely determined, but $L_{D_{\text{opt}}}$ is uniquely determined as in GANs using hinge loss. In such cases, $L_{D,\text{flood},1}$ and $L_{D,\text{flood},2}$, which require low flood levels for $L_{D_{\text{opt}},\text{real}}$ and $L_{D_{\text{opt}},\text{fake}}$, should be avoided. Therefore, the setting b_{all} lower than $L_{D_{\text{opt}}}$ and applying $L_{D,\text{flood},3}$ is the inspiration for Hypothesis 2. Since $L_{D_{\text{opt}}}$ is uniquely determined for BCE losses, $L_{D,\text{flood},3}$ can also be applied. The column, flooding type, in Table 2 indicates appropriate flooding type for each adversarial loss.

To provide theoretical support for Hypotheses 1 and 2, let us consider the case of applying flooding to GANs with BCE loss. For each adversarial loss, $\mathbb{P}_g = \mathbb{P}_r$ at the training convergence is proved following the procedure outlined in Section 2.1. In the early stages of the training, the difference between \mathbb{P}_g and \mathbb{P}_r is more significant, so the loss L_{D^*} is lower than $L_{D_{\text{opt}}}$ because the discriminator can solve the discrimination task well by its distribution difference. For example, Goodfellow et al. [7] showed that for GANs with BCE loss and a fixed generator G ,

$$D^*(\mathbf{x}) = \frac{\mathbb{P}_r(\mathbf{x})}{\mathbb{P}_r(\mathbf{x}) + \mathbb{P}_g(\mathbf{x})}. \quad (10)$$

It can also be proven that $L_{D^*,\text{real}}$ and $L_{D^*,\text{fake}}$ are smaller than $L_{D_{\text{opt}},\text{real}}$ and $L_{D_{\text{opt}},\text{fake}}$. Since $L_{D_{\text{opt}},\text{real}} = L_{D_{\text{opt}},\text{fake}} = \log 2$ with BCE loss, we assume $b_{\text{real}} = b_{\text{fake}}$ in the proof. We can now show the following theorem.

Theorem 1. *In training GANs with BCE loss based on*

$L_{D,\text{flood},1}$ and setting $b \geq \log 2$,

$$D^*(\mathbf{x}) \in \{1 - e^{-b}, e^{-b}\}, \quad (11)$$

where $b = b_{\text{real}} = b_{\text{fake}}$. On the other hand, with setting $b < \log 2$,

$$\begin{cases} D^*(\mathbf{x}) = \frac{\mathbb{P}_r(\mathbf{x})}{\mathbb{P}_r(\mathbf{x}) + \mathbb{P}_g(\mathbf{x})} & \text{if } \mathbb{P}_g(\mathbf{x}) \text{ satisfies} \\ D^*(\mathbf{x}) \in \{1 - e^{-b}, e^{-b}\} & \text{inequality (13),} \\ & \text{otherwise,} \end{cases} \quad (12)$$

where the inequality is

$$1 - e^{-b} < \frac{\mathbb{P}_r(\mathbf{x})}{\mathbb{P}_r(\mathbf{x}) + \mathbb{P}_g(\mathbf{x})} < e^{-b}. \quad (13)$$

Proof. See Supplementary Section A. \square

The theorem is important in the following two points.

1. When $b_{\text{real}} = b_{\text{fake}} \geq \log 2$, the output of D^* becomes a constant, which does not relate to \mathbb{P}_g and \mathbb{P}_r . Then the training will collapse. When $b_{\text{real}} = b_{\text{fake}} < \log 2$, the output of D^* is the same as Eq. (10), then the training converges by $\mathbb{P}_r(\mathbf{x}) = \mathbb{P}_g(\mathbf{x})$.
2. When $b_{\text{real}} = b_{\text{fake}} < \log 2$ and if the flood level approaches $\log 2$, the generator of GANs with a higher flood level is more difficult to satisfy the inequality (13) discussed in Supplementary Section B.

We assume that higher flood levels increase the dangers mentioned above and lower flood levels diminish the stabilizing effect. Therefore, it is necessary to investigate the appropriate setting of the flood level through experiments.

4. Experiment

We show experimentally the appropriate application and the effect of flooding on GANs discussed in Section 3.

4.1. Implementation

We used unconditional DCGAN [25] as the architecture of GANs. Since DCGAN generates images of 64×64 pixels, we added convolutional layers to the discriminator and the generator to deal with 128×128 pixels when we used the CelebA dataset. For the final layer of the discriminator in DCGAN, Radford et al. used a sigmoid layer to convert the output to $(0, 1)$. We excluded the layer when we used adversarial losses that assume an output that takes real values. We followed Radford et al. for batch normalization layers and Miyato et al. [22] for spectral normalization layers. When adding the gradient penalty, the implementation details, such as loss weights, also followed the research of Gulrajani et al. [8] On the other hand, while we primarily followed the methods of Arjovsky et al. [2], we adopted 0.1 as the clipping parameter c , since the recommended parameter $c = 0.1$ doesn't work well regardless of whether flooding was applied to our experiments. The batch size

Type	Small	Medium	Opt- ε	Opt	Over Opt
$L_{D,\text{flood},1}, L_{D,\text{flood},2}$	ε_1	$L_{D_{\text{opt,real}}}/2$	$L_{D_{\text{opt,real}}} - \varepsilon_1$	$L_{D_{\text{opt,real}}}$	$L_{D_{\text{opt,real}}} + 0.5$
$L_{D,\text{flood},3}$	ε_2	$L_{D_{\text{opt}}}/2$	$L_{D_{\text{opt}}} - \varepsilon_2$	$L_{D_{\text{opt}}}$	$L_{D_{\text{opt}}} + 1.0$
$L_{D,\text{flood},3}$ (WGAN)	-1.0	-0.5	$-\varepsilon_2$	0.0	1.0

Table 3. Flood level settings for each experiment. The first row represents settings of b_{real} . The second and third rows show the settings of b_{all} . We adopt $(\varepsilon_1, \varepsilon_2) = (0.05, 0.1)$.

Flooding type	w/o flooding	Small	Medium	Opt- ε	Opt	Over Opt
$L_{D,\text{flood},1}$	281.0 (136.8)	71.4 (3.3)	131.9 (97.6)	146.4 (139.7)	446.6 (31.6)	371.4 (101.9)
$L_{D,\text{flood},2}$	—	83.5 (22.7)	67.0 (2.0)	73.1 (5.6)	284.0 (35.9)	416.6 (48.2)
$L_{D,\text{flood},3}$	—	71.0 (5.4)	63.6 (3.6)	65.6 (3.1)	109.1 (10.7)	408.9 (41.9)

Table 4. Average (standard deviation) of FID with non-saturating BCE loss, different flooding types, and flood levels.

was 128, the learning rate was 0.0002, and Adam optimizer ($\beta = (0.5, 0.999)$) was employed. The training used one GPU for 100,000 iterations. We conducted each experiment five times, and the generated images were evaluated using Fréchet Inception Distance (FID) [9].

4.2. How to apply flooding

First, we investigated the stabilizing effect of the basic GAN training by flooding and determined which type in Eq. (7) is appropriate. We used non-saturating BCE loss and did not use any regularization term. Note that the discussion in Section 3.2.1 does not use $f_G = \log(1 - D(G(z)))$, and we can make the same arguments with non-saturating BCE loss. To compare a case without flooding and cases with flooding and to find the appropriate flood level, we conducted experiments on five different settings (Small, Medium, Opt- ε , Opt, Over opt). For the flood level b_{real} in the flooding types 1 and 2, we tried five different settings of the flood level in Table 3, and we use b_{fake} calculated from Table 3 which replace $b_{D_{\text{opt,real}}}$ to $b_{D_{\text{opt,real}}}$. We examined the flood level b_{all} in flooding type 3 for five different flood level settings in Table 3.

Table 4 shows the average and standard deviation of the FID scores with CIFAR10. From comparing results with flood level Small, Medium, and Opt- ε with results without flooding, we observe that applying flooding to GANs stabilizes the training. The discriminator with flooding avoids taking losses below the flood level. The results indicate that a discriminator can avoid losses below $L_{D_{\text{opt,real}}}$, $L_{D_{\text{opt,fake}}}$, and $L_{D_{\text{opt}}}$ during the training GANs and that the training becomes unstable when the loss is too low. We can also see that the training completely collapses when the flood level $b_{\text{real}}, b_{\text{fake}}, b_{\text{all}}$ takes $L_{D_{\text{opt,real}}}, L_{D_{\text{opt,fake}}}, L_{D_{\text{opt}}}$ or more. Compared with the results without flooding, the collapse of the generated images with flooding level Opt and Over Opt started early on, as shown in Figure 2, indicating that such a configuration disrupts the GAN training. It matches the discussion in Section 3.2.2. The stabiliza-

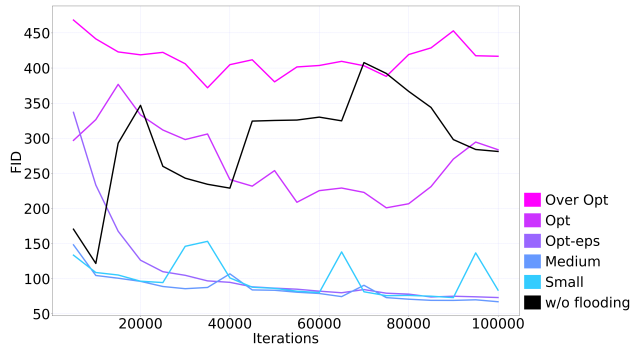


Figure 2. Relationship between flood levels and FID transition. Results with flood level Small, Medium, and Opt- ε are more stable than those without flooding. On the other hand, experiments with flood level Opt and Over Opt collapse from the beginning.

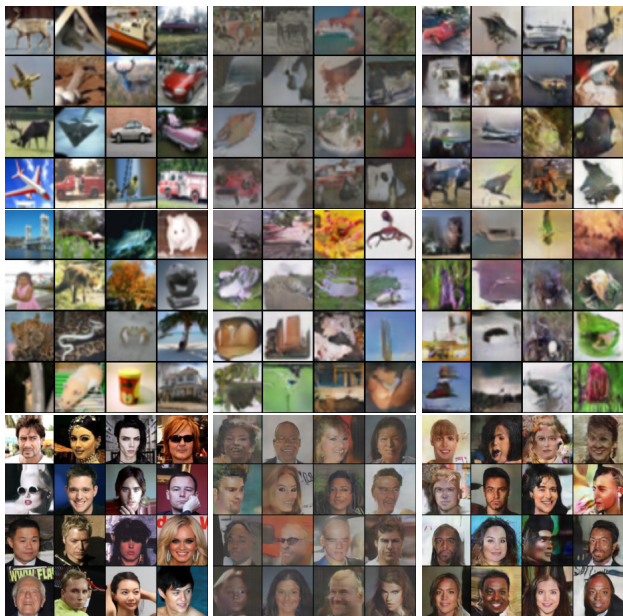
tion effect was confirmed for all three flooding types by setting Small, Medium, and Opt- ε flood levels. Moreover, the overall score is better for flooding type 2 than for flooding type 1. It suggests that inserting flooding for the overall loss per batch, rather than the loss for each image, is more effective. Also, it is worth noting that the flood level Medium and Opt- ε stabilize the training. It suggests that GAN training can progress even if the discriminator loses its ability to take low losses and also implies that a low discriminator loss may destabilize training. As shown in Theorem 1, setting a larger flood level reduces the probability of satisfying the inequality (13). However, the experimental result suggests that preventing destabilization is more beneficial than that in this experiment. We provide analysis on the loss and gradient with flooding in Supplementary Section D.

4.3. Flooding for various losses and datasets

Flooding effects for various adversarial losses Next, we examined the effect of flooding on various adversarial losses: BCE loss (non-saturating), Wasserstein loss, hinge loss, and least squares loss. we use DCGAN and CIFAR10, and do not use any regularization term. We adopted the fol-

Adversarial loss	w/o flooding	Small	Medium	Opt- ϵ	Opt	Over Opt
BCE loss (non-saturating)	281.0 (136.8)	83.5 (22.7)	67.0 (2.0)	73.1 (5.6)	284.0 (35.9)	416.6 (48.2)
Wasserstein loss	82.6 (9.7)	79.2 (6.2)	72.0 (3.9)	78.5 (5.4)	386.8 (24.0)	462.9 (19.3)
Hinge loss	148.0 (62.3)	76.1 (6.2)	66.3 (3.6)	77.0 (7.5)	316.7 (42.0)	451.5 (24.9)
Least squares loss	118.7 (63.5)	107.9 (83.8)	66.7 (2.5)	63.6 (3.9)	184.6 (14.5)	457.0 (20.1)

Table 5. Results with each flood level for each adversarial loss. We show the score information as “average FID (standard deviation).”



(a) Training images (b) Without flooding (c) With flooding

Figure 3. Comparison of generated images when experimented with datasets (CIFAR10 (top), CIFAR100 (middle), and CelebA (bottom)) and non-saturating BCE loss. Taking the result with CIFAR10 as an example, compared to the training images (a), when the training without flooding becomes unstable, the generated image gradually collapses, for example, the graying ((b), FID: 107.3). In contrast, if flooding is applied at the appropriate flood level, the generated images are not collapsed, as shown in ((c), FID: 63.4). If the flood level is too high, the training and the generated images collapse from the beginning.

lowing policy for selecting flooding types.

1. When we can use any one of the flooding types (1,2,3) in Table 2, we use flooding type 2 with Table 3 setting.
2. When we can only apply flooding type 3 in Table 2, we use flooding type 3 with the setting in Table 3.

Note that we treat the flood levels for Wasserstein loss separately as shown in Table 3 since $L_{D_{\text{opt}}} = 0$.

Table 5 shows the average and standard deviation of the FID scores using the four adversarial losses. The results show that the combination of flooding and the change in the type of adversarial loss further stabilizes the training. We can also make the same argument for the relationship between the flood level b_{real} , b_{fake} , b_{all} and $L_{D_{\text{opt},\text{real}}}$,

Adversarial loss	w/o smoothing	w smoothing
BCE loss (non-saturating)	281.0 (136.8)	74.5 (23.6)
Wasserstein loss	82.6 (9.7)	182.1 (142.6)
Hinge loss	148.0 (62.3)	67.7 (3.4)
Least squares loss	118.7 (63.5)	109.5 (17.3)

Table 6. Results with or without label smoothing for each adversarial loss. We show the score information as “average FID (standard deviation).”

$L_{D_{\text{opt},\text{fake}}}$, $L_{D_{\text{opt}}}$ as Section 4.2. Furthermore, the results support Hypotheses 1 and 2. Also, overall, the results were best when the flooding setting was Medium. It suggests that we need the right amount of flood: with a flood level that is too small, we will not have the expected stabilizing effect, and with a flood level that is too close to Opt, it will unfortunately lead to instability.

Next, we compared the effect of flooding and label smoothing on various adversarial losses. Label smoothing and the proposed method share similarities as stabilization techniques that do not add regularization terms while preserving the type of adversarial losses. We adopted one-sided label smoothing and calculated $L_{D_{\text{real}}}$ with $a = 0.9$,

$$L_{D_{\text{real}}} = \mathbb{E}_{\mathbf{x} \sim \mathbb{P}_r} [a \cdot f_{D_{\text{real}}}(D(\mathbf{x})) + (1 - a) \cdot f_{D_{\text{fake}}}(D(\mathbf{x}))]. \quad (14)$$

Table 6 shows that the effect of label smoothing is not consistently confirmed except for non-saturating BCE loss and hinge loss and that it rather worsens the performance for Wasserstein loss. As shown in Table 5, flooding is superior in that it can be combined with various losses.

Flooding effects for various datasets Next, we verified whether flooding provides stabilization regardless of the dataset. We conducted experiments on MNIST, Fashion-MNIST, CIFAR100, and CelebA, with DCGAN, non-saturating BCE loss, and flood level Medium.

We show the results in Table 7 and the generated images in Figure 3. Although the difficulty of the image generation task is different among the datasets, the results show that flooding is effective on various datasets.

4.4. Flooding with other techniques

Additional regularization terms and architectural changes can be used to stabilize the GAN training. We examined the effects of flooding in combination with

Dataset	w/o flooding	w flooding
CIFAR10	281.0 (136.8)	67.0 (2.0)
MNIST	297.2 (135.9)	70.9 (10.9)
Fashion-MNIST	133.0 (126.6)	67.2 (10.2)
CIFAR100	343.8 (139.1)	64.5 (4.0)
CelebA	312.3(134.1)	129.9 (138.5)

Table 7. FID for each dataset with or without flooding. We show the score information as “average FID (standard deviation).”

Type	w/o flooding	w flooding
DCGAN	281.0 (136.8)	67.0 (2.0)
DCGAN(2x)	188.7 (153.3)	62.9 (4.7)
DCGAN(4x)	334.4 (140.9)	61.6 (4.5)
SNDCGAN	49.1 (1.2)	47.9 (2.0)
SNDCGAN (hinge loss)	53.5 (1.8)	51.5 (1.6)
Gradient penalty	60.7 (8.1)	50.9 (1.7)
WGAN	82.6 (9.7)	72.0 (3.9)
WGAN-GP	85.0 (4.1)	72.5 (5.4)
WGAN (clipping)	77.7 (10.5)	72.1 (6.9)

Table 8. FID with or without in combination with the addition of a regularization term or change of the architecture. We show the score information as “average FID (standard deviation).”

Application	w/o flooding	w flooding
CDCGAN	195.4 (45.5)	130.0 (51.9)
ADDA	0.517 (0.09)	0.698 (0.08)

Table 9. Results with or without in combination with various adversarial frameworks. We show the score information as “average FID (standard deviation)” for CDCGAN with CIFAR10. We also provide “domain accuracy (standard deviation)” for ADDA with source domain (MNIST) and target domain (MNIST-M).

spectral normalization and gradient penalty, commonly used as improvement methods, on DCGAN. Moreover, since spectral normalization is often used with hinge loss, and gradient penalty is typically employed with WGAN, we also investigated the effect of flooding in these cases (SNDCGAN (hinge loss) and WGAN-GP). We also conducted experiments with WGAN and weight clipping to assess how flooding influences this setup. In addition, we conducted experiments by increasing the feature size in the generator’s intermediate layer (DCGAN (2x), DCGAN (4x)) to verify the effect of flooding even when the model size changes. We used CIFAR10 as the dataset.

Table 8 shows the results. The results show that flooding stabilizes training regardless of the model size, although instability exists. It supports the versatility of flooding in GANs, which have a wide range of types and sizes of models. The results also demonstrate that using spectral normalization and flooding together improves the performance. Moreover, flooding improves the performance in the case of gradient penalty and weight clipping.

4.5. Flooding with other adversarial application

We examined the effects of flooding with other adversarial applications, such as conditional GANs and domain adaptation. For the experiments of conditional GANs, we conduct experiments with conditional DCGAN (CDCGAN) and CIFAR10. Mirza et al. [21] proposed the loss for conditional GANs with BCE loss. Therefore, we adopt the strategy as Sections 4.3 and 4.4 when applying flooding. To verify the effects of flooding on adversarial learning for domain adaptation, we used adversarial discriminative domain adaptation (ADDA) [30] and conducted experiments with MNIST (source domain) and MNIST-M (target domain). We describe the definition of loss with flooding for ADDA in Supplementary Section E.

We provided the result in Table 9. The results demonstrate that flooding improves the performance of both of CDCGAN and ADDA. Therefore, it is suggested that flooding can be applied in a wide range of adversarial applications to increase performance.

4.6. Limitations

While flooding demonstrates stabilization effects in the training of various GANs, we observed collapsed results with CelebA. It should be noted that flooding cannot prevent all instabilities of GAN training. For example, ensuring Lipschitz continuity to regularize gradients is the focus of well-known existing methods, such as gradient penalty and spectral normalization; however, it is beyond the scope of our approach. Therefore, flooding should be combined with other stabilization techniques appropriately based on the instability to be prevented.

5. Conclusion and future work

We proposed to apply flooding, a method for preventing overfitting in supervised learning, to GANs. Although our proposed method has an additional hyperparameter b , we demonstrated how we consider a range for the flood level values. We support the proposal through the theoretical analysis of the relationship between the flood level and the distribution of generated images. The stabilization effects of flooding and the proposal’s validity were demonstrated through experiments. We also showed that flooding is effective when combined with existing training stabilization methods, such as changes in the type of adversarial losses and architectural changes.

Further investigation is necessary to understand why GAN training with flooding can progress stably. The effect of flooding on SoTA models also needs to be verified.

Disclaimer We used Grammarly to fix typos and grammar issues. We used ChatGPT and DeepL to edit part of the sentences in this manuscript.

References

- [1] Martin Arjovsky and Leon Bottou. Towards principled methods for training generative adversarial networks. In *ICLR*, 2017. 1, 2
- [2] Martin Arjovsky, Soumith Chintala, and Léon Bottou. Wasserstein generative adversarial networks. In *ICML*, 2017. 2, 3, 5
- [3] Andrew Brock, Jeff Donahue, and Karen Simonyan. Large scale GAN training for high fidelity natural image synthesis. In *ICLR*, 2019. 3, 4
- [4] Tong Che, Yanran Li, Athul Jacob, Yoshua Bengio, and Wenjie Li. Mode regularized generative adversarial networks. In *ICLR*, 2017. 3
- [5] Ugur Demir and Gözde B. Ünal. Patch-based image inpainting with generative adversarial networks. *arXiv preprint arXiv:1803.07422*, 2018. 1
- [6] Yaroslav Ganin, Evgeniya Ustinova, Hana Ajakan, Pascal Germain, Hugo Larochelle, François Laviolette, Mario March, and Victor Lempitsky. Domain-adversarial training of neural networks. *Journal of Machine Learning Research*, 17(59):1–35, 2016. 4
- [7] Ian Goodfellow, Jean Pouget-Abadie, Mehdi Mirza, Bing Xu, David Warde-Farley, Sherjil Ozair, Aaron Courville, and Yoshua Bengio. Generative adversarial nets. In *NeurIPS*, 2014. 1, 2, 3, 4, 5
- [8] Ishaan Gulrajani, Faruk Ahmed, Martin Arjovsky, Vincent Dumoulin, and Aaron C Courville. Improved training of wasserstein GANs. In *NeurIPS*, 2017. 2, 3, 5
- [9] Martin Heusel, Hubert Ramsauer, Thomas Unterthiner, Bernhard Nessler, and Sepp Hochreiter. Gans trained by a two time-scale update rule converge to a local nash equilibrium. In *NeurIPS*, 2017. 6
- [10] Sergey Ioffe and Christian Szegedy. Batch normalization: Accelerating deep network training by reducing internal covariate shift. In *ICML*, 2015. 4
- [11] Takashi Ishida, Ikko Yamane, Tomoya Sakai, Gang Niu, and Masashi Sugiyama. Do we need zero training loss after achieving zero training error? In *ICML*, 2020. 2, 4
- [12] Phillip Isola, Jun-Yan Zhu, Tinghui Zhou, and Alexei A. Efros. Image-to-image translation with conditional adversarial networks. In *CVPR*, 2017. 4
- [13] Tero Karras, Timo Aila, Samuli Laine, and Jaakko Lehtinen. Progressive growing of GANs for improved quality, stability, and variation. In *ICLR*, 2018. 4
- [14] Tero Karras, Samuli Laine, and Timo Aila. A style-based generator architecture for generative adversarial networks. In *CVPR*, 2019. 4
- [15] Tero Karras, Samuli Laine, Miika Aittala, Janne Hellsten, Jaakko Lehtinen, and Timo Aila. Analyzing and improving the image quality of stylegan. In *CVPR*, 2020. 4
- [16] Naveen Kodali, Jacob D. Abernethy, James Hays, and Zsolt Kira. How to train your DRAGAN. *CoRR*, abs/1705.07215, 2017. 3
- [17] C. Ledig, L. Theis, F. Huszar, J. Caballero, A. Cunningham, A. Acosta, A. Aitken, A. Tejani, J. Totz, Z. Wang, and W. Shi. Photo-realistic single image super-resolution using a generative adversarial network. In *CVPR*, 2017. 1
- [18] Ziqiang Li, Muhammad Usman, Rentuo Tao, Pengfei Xia, Chaoyue Wang, Huanhuan Chen, and Bin Li. A systematic survey of regularization and normalization in gans. *ACM Comput. Surv.*, 55(11), 2023. 4
- [19] Jae Hyun Lim and Jong Chul Ye. Geometric gan. *arXiv preprint arXiv:1705.02894*, 2017. 2, 3
- [20] Xudong Mao, Qing Li, Haoran Xie, Raymond Y.K. Lau, Zhen Wang, and Stephen Paul Smolley. Least squares generative adversarial networks. In *ICCV*, 2017. 2, 3
- [21] Mehdi Mirza and Simon Osindero. Conditional generative adversarial nets. *arXiv preprint arXiv:1411.1784*, 2014. 4, 8
- [22] Takeru Miyato, Toshiki Kataoka, Masanori Koyama, and Yuichi Yoshida. Spectral normalization for generative adversarial networks. In *ICLR*, 2018. 2, 3, 5
- [23] Taesung Park, Ming-Yu Liu, Ting-Chun Wang, and Jun-Yan Zhu. Semantic image synthesis with spatially-adaptive normalization. In *CVPR*, 2019. 1
- [24] Henning Petzka, Asja Fischer, and Denis Lukovnikov. On the regularization of wasserstein GANs. In *ICLR*, 2018. 3
- [25] Alec Radford, Luke Metz, and Soumith Chintala. Unsupervised representation learning with deep convolutional generative adversarial networks. *arXiv preprint arXiv:1511.06434*, 2016. 4, 5
- [26] Tim Salimans, Ian Goodfellow, Wojciech Zaremba, Vicki Cheung, Alec Radford, Xi Chen, and Xi Chen. Improved techniques for training GANs. In *NeurIPS*, 2016. 1, 2, 3
- [27] Connor Shorten and Taghi M. Khoshgoufar. A survey on image data augmentation for deep learning. *Journal of Big Data*, 6(1):60, 2019. 4
- [28] Nitish Srivastava, Geoffrey Hinton, Alex Krizhevsky, Ilya Sutskever, and Ruslan Salakhutdinov. Dropout: A simple way to prevent neural networks from overfitting. *Journal of Machine Learning Research*, 15(56):1929–1958, 2014. 4
- [29] Christian Szegedy, Vincent Vanhoucke, Sergey Ioffe, Jon Shlens, and Zbigniew Wojna. Rethinking the inception architecture for computer vision. In *CVPR*, 2016. 4
- [30] Eric Tzeng, Judy Hoffman, Kate Saenko, and Trevor Darrell. Adversarial discriminative domain adaptation. In *CVPR*, 2017. 4, 8
- [31] Zhengwei Wang, Qi She, and Tomás E. Ward. Generative adversarial networks in computer vision: A survey and taxonomy. *ACM Comput. Surv.*, 54(2), feb 2021. 1, 2, 3
- [32] Sitao Xiang and Hao Li. On the effects of batch and weight normalization in generative adversarial networks. *arXiv preprint arXiv:1704.03971*, 2017. 3
- [33] Han Zhang, Ian Goodfellow, Dimitris Metaxas, and Augustus Odena. Self-attention generative adversarial networks. In *ICML*, 2019. 4
- [34] Han Zhang, Tao Xu, Hongsheng Li, Shaoting Zhang, Xiaogang Wang, Xiaolei Huang, and Dimitris Metaxas. Stackgan: Text to photo-realistic image synthesis with stacked generative adversarial networks. In *ICCV*, 2017. 4
- [35] Jun-Yan Zhu, Taesung Park, Phillip Isola, and Alexei A Efros. Unpaired image-to-image translation using cycle-consistent adversarial networks. In *ICCV*, 2017. 1

Supplementary

A. Proof of Theorem 1

Theorem 1. In training GANs with BCE loss based on $L_{D,\text{flood},1}$ and setting $b \geq \log 2$,

$$D^*(\mathbf{x}) \in \{1 - e^{-b}, e^{-b}\}, \quad (15)$$

where $b = b_{\text{real}} = b_{\text{fake}}$. On the other hand, with setting $b < \log 2$,

$$\begin{cases} D^*(\mathbf{x}) = \frac{\mathbb{P}_r(\mathbf{x})}{\mathbb{P}_r(\mathbf{x}) + \mathbb{P}_g(\mathbf{x})} & \text{if } \mathbb{P}_g(\mathbf{x}) \text{ satisfies} \\ & \text{inequality (17),} \\ D^*(\mathbf{x}) \in \{1 - e^{-b}, e^{-b}\} & \text{otherwise,} \end{cases} \quad (16)$$

where the inequality is

$$1 - e^{-b} < \frac{\mathbb{P}_r(\mathbf{x})}{\mathbb{P}_r(\mathbf{x}) + \mathbb{P}_g(\mathbf{x})} < e^{-b}. \quad (17)$$

First, we show a lemma before the proof.

Lemma 2. If $a \geq 0$ and $b \geq 0$ and $a \neq b$, the following inequality is not satisfied,

$$0 < \frac{a}{a-b} < 1. \quad (18)$$

Proof. We will prove it by contradiction. If a and b satisfy the inequality, $a - b > 0$ is also satisfied. Therefore, we have

$$\begin{aligned} \frac{a}{a-b} &< 1 \\ \Rightarrow a &< a - b \\ \Rightarrow b &< 0. \end{aligned} \quad (19)$$

However, it contradicts the assumption $b \geq 0$. \square

Proof. The discriminator loss $L_{D,\text{flood},1}$ with BCE loss is expressed as

$$\begin{aligned} L_{D,\text{flood},1} &= \mathbb{E}_{\mathbf{x} \sim \mathbb{P}_r} [h(f_{D,\text{real}}(D(\mathbf{x})), b)] \\ &\quad + \mathbb{E}_{\mathbf{x} \sim \mathbb{P}_g} [h(f_{D,\text{fake}}(D(\mathbf{x})), b)] \\ &= \mathbb{E}_{\mathbf{x} \sim \mathbb{P}_r} [h(-\log(D(\mathbf{x})), b)] \\ &\quad + \mathbb{E}_{\mathbf{x} \sim \mathbb{P}_g} [h(-\log(1 - D(\mathbf{x})), b)] \\ &= \int \mathbb{P}_r(\mathbf{x}) [h(-\log(D(\mathbf{x})), b)] \\ &\quad + \mathbb{P}_g(\mathbf{x}) [h(-\log(1 - D(\mathbf{x})), b)] d\mathbf{x}. \end{aligned} \quad (20)$$

We introduce $f(D(\mathbf{x}))$ to examine the relationship between D and $L_{D,\text{flood},1}$ shown as

$$f(D(\mathbf{x})) = \mathbb{P}_r(\mathbf{x}) [h(-\log(D(\mathbf{x})), b)] + \mathbb{P}_g(\mathbf{x}) [h(-\log(1 - D(\mathbf{x})), b)]. \quad (21)$$

We demonstrate minimization of $f(D(\mathbf{x}))$ in two cases with respect to b and $\log 2$.

Case 1. If the flood level satisfies $b > \log 2$, b satisfies

$$e^{-b} < 1 - e^{-b}. \quad (22)$$

We divide $D(\mathbf{x}) \in (0, 1)$ to three intervals with respect to e^{-b} and $1 - e^{-b}$.

Case 1(a). If we assume $0 < D(\mathbf{x}) \leq e^{-b}$, we can transform $f(D(\mathbf{x}))$ as

$$f(D(\mathbf{x})) = \mathbb{P}_r(\mathbf{x}) [-\log(D(\mathbf{x}))] + \mathbb{P}_g(\mathbf{x}) [\log(1 - D(\mathbf{x})) + 2b]. \quad (23)$$

Therefore, the derivative with respect to $D(\mathbf{x})$ is expressed as

$$f'(D(\mathbf{x})) = -\frac{\mathbb{P}_r(\mathbf{x})}{D(\mathbf{x})} - \frac{\mathbb{P}_g(\mathbf{x})}{1 - D(\mathbf{x})}. \quad (24)$$

Now, we can obtain $D(\mathbf{x})$ where $f'(D(\mathbf{x})) = 0$ as

$$D(\mathbf{x}) = \frac{\mathbb{P}_r(\mathbf{x})}{\mathbb{P}_r(\mathbf{x}) - \mathbb{P}_g(\mathbf{x})}, \quad (25)$$

if it can be defined ($\mathbb{P}_r(\mathbf{x}) \neq \mathbb{P}_g(\mathbf{x})$). Because the probability distribution $\mathbb{P}_r(\mathbf{x})$ and $\mathbb{P}_g(\mathbf{x})$ have non-negative values, $D(\mathbf{x})$ shown in Eq. (25) never satisfies $0 < D(\mathbf{x}) < 1$ shown as Lemma 2. Therefore, $f(D(\mathbf{x}))$ in the interval $0 < D(\mathbf{x}) \leq e^{-b}$ monotonically decrease, and $D(\mathbf{x}) = e^{-b}$ gives the minimum of $f(D(\mathbf{x}))$ in the interval.

Case 1(b). If we assume $e^{-b} \leq D(\mathbf{x}) \leq 1 - e^{-b}$, we can obtain $f(D(\mathbf{x}))$ and $f'(D(\mathbf{x}))$ as

$$\begin{aligned} f(D(\mathbf{x})) &= \mathbb{P}_r(\mathbf{x}) [\log(D(\mathbf{x})) + 2b] \\ &\quad + \mathbb{P}_g(\mathbf{x}) [\log(1 - D(\mathbf{x})) + 2b], \\ f'(D(\mathbf{x})) &= \frac{\mathbb{P}_r(\mathbf{x})}{D(\mathbf{x})} - \frac{\mathbb{P}_g(\mathbf{x})}{1 - D(\mathbf{x})}. \end{aligned} \quad (26)$$

Now, we can obtain $D(\mathbf{x})$ where $f'(D(\mathbf{x})) = 0$ as

$$D(\mathbf{x}) = \frac{\mathbb{P}_r(\mathbf{x})}{\mathbb{P}_r(\mathbf{x}) + \mathbb{P}_g(\mathbf{x})}. \quad (27)$$

Moreover, $f'(e^{-b})$ and $f'(1 - e^{-b})$ are expressed as

$$\begin{aligned} f'(e^{-b}) &= \frac{\mathbb{P}_r(\mathbf{x})}{e^{-b}} - \frac{\mathbb{P}_g(\mathbf{x})}{1 - e^{-b}} \\ &= \frac{(1 - e^{-b})\mathbb{P}_r(\mathbf{x}) - e^{-b}\mathbb{P}_g(\mathbf{x})}{e^{-b}(1 - e^{-b})} \\ &= \frac{\mathbb{P}_r(\mathbf{x}) - e^{-b}(\mathbb{P}_r(\mathbf{x}) + \mathbb{P}_g(\mathbf{x}))}{e^{-b}(1 - e^{-b})}, \\ f'(1 - e^{-b}) &= \frac{\mathbb{P}_r(\mathbf{x})}{1 - e^{-b}} - \frac{\mathbb{P}_g(\mathbf{x})}{e^{-b}} \\ &= \frac{e^{-b}\mathbb{P}_r(\mathbf{x}) - (1 - e^{-b})\mathbb{P}_g(\mathbf{x})}{e^{-b}(1 - e^{-b})} \\ &= \frac{\mathbb{P}_r(\mathbf{x}) - (1 - e^{-b})(\mathbb{P}_r(\mathbf{x}) + \mathbb{P}_g(\mathbf{x}))}{e^{-b}(1 - e^{-b})}. \end{aligned} \quad (28)$$

If $\mathbb{P}_g(\mathbf{x})$ satisfies inequality

$$e^{-b} < \frac{\mathbb{P}_r(\mathbf{x})}{\mathbb{P}_r(\mathbf{x}) + \mathbb{P}_g(\mathbf{x})} < 1 - e^{-b}, \quad (29)$$

we obtain $f'(e^{-b}) > 0$ and $f'(1 - e^{-b}) < 0$. Therefore, $D(\mathbf{x}) \in \{1 - e^{-b}, e^{-b}\}$ gives the minimum. If $\mathbb{P}_g(\mathbf{x})$ doesn't satisfy the inequality, $f(D(\mathbf{x}))$ monotonically increase or decrease in the interval, and $D(\mathbf{x}) \in \{1 - e^{-b}, e^{-b}\}$ gives the minimum.

Case 1(c). If we assume $1 - e^{-b} \leq D(\mathbf{x}) < 1$, we can obtain $f(D(\mathbf{x}))$ and $f'(D(\mathbf{x}))$ as

$$\begin{aligned} f(D(\mathbf{x})) &= \mathbb{P}_r(\mathbf{x})[\log(D(\mathbf{x})) + 2b] \\ &\quad + \mathbb{P}_g(\mathbf{x})[-\log(1 - D(\mathbf{x}))], \\ f'(D(\mathbf{x})) &= \frac{\mathbb{P}_r(\mathbf{x})}{D(\mathbf{x})} + \frac{\mathbb{P}_g(\mathbf{x})}{1 - D(\mathbf{x})}, \end{aligned} \quad (30)$$

and we have $D(\mathbf{x})$ that satisfies $f'(D(\mathbf{x})) = 0$ as

$$D(\mathbf{x}) = \frac{\mathbb{P}_r(\mathbf{x})}{\mathbb{P}_r(\mathbf{x}) - \mathbb{P}_g(\mathbf{x})}, \quad (31)$$

if it can be defined ($\mathbb{P}_r(\mathbf{x}) \neq \mathbb{P}_g(\mathbf{x})$). As Case 1(a), the $D(\mathbf{x})$ doesn't exist in the interval. Therefore, $f(D(\mathbf{x}))$ monotonically increase, and $D(\mathbf{x}) = 1 - e^{-b}$ gives the minimum of $f(D(\mathbf{x}))$ in the interval.

Finally, from Case 1(a), 1(b), and 1(c), we can prove Eq. (15).

Case 2. If the flood level satisfies $b \leq \log 2$, b satisfies

$$1 - e^{-b} < e^{-b}, \quad (32)$$

and we can divide $(0, 1)$ to three intervals with respect to $1 - e^{-b}$ and e^{-b} .

Case 2(a). If we assume $0 < D(\mathbf{x}) \leq 1 - e^{-b}$, we have

$$\begin{aligned} f(D(\mathbf{x})) &= \mathbb{P}_r(\mathbf{x})[-\log(D(\mathbf{x}))] \\ &\quad + \mathbb{P}_g(\mathbf{x})[\log(1 - D(\mathbf{x})) + 2b], \\ f'(D(\mathbf{x})) &= -\frac{\mathbb{P}_r(\mathbf{x})}{D(\mathbf{x})} - \frac{\mathbb{P}_g(\mathbf{x})}{1 - D(\mathbf{x})}. \end{aligned} \quad (33)$$

As Case 1(a), there is no $D(\mathbf{x})$ that $f'(D(\mathbf{x})) = 0$ in the interval. Therefore, $D(\mathbf{x}) = 1 - e^{-b}$ gives the minimum of $f(D(\mathbf{x}))$ in the interval.

Case 2(b). If we assume $1 - e^{-b} \leq D(\mathbf{x}) \leq e^{-b}$, we have

$$\begin{aligned} f(D(\mathbf{x})) &= \mathbb{P}_r(\mathbf{x})[-\log(D(\mathbf{x}))] \\ &\quad + \mathbb{P}_g(\mathbf{x})[-\log(1 - D(\mathbf{x}))], \\ f'(D(\mathbf{x})) &= -\frac{\mathbb{P}_r(\mathbf{x})}{D(\mathbf{x})} + \frac{\mathbb{P}_g(\mathbf{x})}{1 - D(\mathbf{x})}. \end{aligned} \quad (34)$$

Therefore, $D(\mathbf{x}) = \frac{\mathbb{P}_r(\mathbf{x})}{\mathbb{P}_r(\mathbf{x}) + \mathbb{P}_g(\mathbf{x})}$ gives $f'(D(\mathbf{x})) = 0$ and satisfies $0 < D(\mathbf{x}) < 1$. We can calculate $f'(1 - e^{-b})$ and $f'(e^{-b})$ as Eq. (28). If $\mathbb{P}_g(\mathbf{x})$ satisfies inequality

$$1 - e^{-b} < \frac{\mathbb{P}_r(\mathbf{x})}{\mathbb{P}_r(\mathbf{x}) + \mathbb{P}_g(\mathbf{x})} < e^{-b}, \quad (35)$$

we obtain $f'(1 - e^{-b}) < 0$ and $f'(e^{-b}) > 0$. Therefore, $D(\mathbf{x}) = \frac{\mathbb{P}_r(\mathbf{x})}{\mathbb{P}_r(\mathbf{x}) + \mathbb{P}_g(\mathbf{x})}$ gives the minimum in the interval.

On the other hand, if $\mathbb{P}_g(\mathbf{x})$ doesn't satisfy the inequality, $f(D(\mathbf{x}))$ monotonically increase or decrease, and $D(\mathbf{x}) \in \{1 - e^{-b}, e^{-b}\}$ gives the minimum in the interval.

Case 2(c). If we assume $e^{-b} \leq D(\mathbf{x}) < 1$, we have

$$\begin{aligned} f(D(\mathbf{x})) &= \mathbb{P}_r(\mathbf{x})[\log(D(\mathbf{x})) + 2b] \\ &\quad + \mathbb{P}_g(\mathbf{x})[-\log(1 - D(\mathbf{x}))], \\ f'(D(\mathbf{x})) &= \frac{\mathbb{P}_r(\mathbf{x})}{D(\mathbf{x})} + \frac{\mathbb{P}_g(\mathbf{x})}{1 - D(\mathbf{x})}. \end{aligned} \quad (36)$$

Now, we can see that there is no $D(\mathbf{x})$ that gives $f'(D(\mathbf{x})) = 0$ in the interval, and $f'(D(\mathbf{x}))$ monotonically increase. Therefore, $D(\mathbf{x}) = e^{-b}$ gives the minimum of $f(D(\mathbf{x}))$ in the interval.

Finally, from Case 2(a), 2(b), and 2(c), we can prove Eq. (16). \square

B. Analysis of Theorem 1

If and only if $\mathbb{P}_g(\mathbf{x})$ satisfies inequality (13), which assumes $b < \log 2$,

$$\mathbb{P}_g(\mathbf{x}) \in \left(\left(\frac{1}{e^{-b}} - 1 \right) \mathbb{P}_r(\mathbf{x}), \left(\frac{1}{1 - e^{-b}} - 1 \right) \mathbb{P}_r(\mathbf{x}) \right). \quad (37)$$

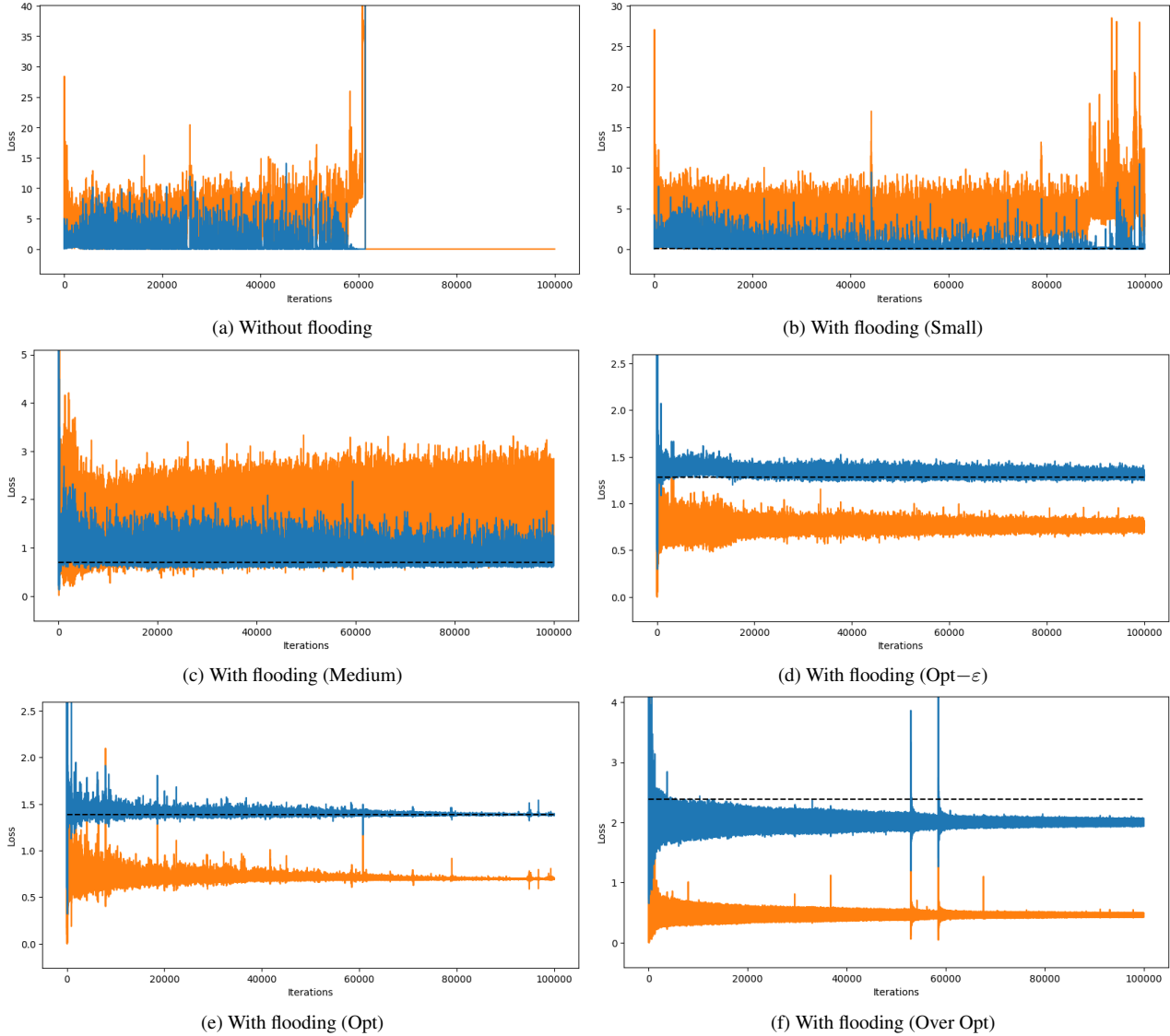


Figure 4. Transition of losses of the generator (orange) and discriminator (blue). The dashed line (black) expresses the flood level for the discriminator. Note that the discriminator’s loss shown in the figure is that before applying flooding.

We will refer to the interval as $I(\mathbb{P}_r(\mathbf{x}), b)$ and then obtain

$$b_0 \leq b_1 \Rightarrow I(\mathbb{P}_r(\mathbf{x}), b_0) \supseteq I(\mathbb{P}_r(\mathbf{x}), b_1). \quad (38)$$

From this perspective, the generator of GANs with higher flood level is more difficult to satisfy the inequality (13).

C. Code implementation

We mainly referred to the following codes and customized them to conduct experiments with various losses and models.

- DCGAN: https://github.com/pytorch/tutorials/blob/main/beginner_source/dcgan_faces_tutorial.py

- FID: <https://github.com/mseitzer/pytorch-fid>

- ADDA: <https://github.com/jvanvugt/pytorch-domain-adaptation>

D. Analysis on the loss and gradient

We showed experimentally that flooding stabilizes GAN training. However, it is unknown why GAN training with flooding succeeds well even when flooding prevents the discriminator’s loss from becoming low. For instance, the flood level Medium is not too low, but GAN training with the flood level was stable rather than collapsed. We conducted additional experiments with BCE loss (non-



Figure 5. Enlarged image of Figure 4. We depicts losses transition of the generator (orange) and discriminator (blue). The dashed line (black) expresses the flood level for the discriminator. Note that the discriminator’s loss shown in the figure is that before applying flooding.

saturating) and $L_{D,\text{flood},2}$ and examined the loss of the generator and the discriminator during the training to understand the training transition of the two models.

The results are provided in Figure 4. We can see that the discriminator’s loss with flooding often shifts over the flood level when the flood level is not too high. Moreover, the losses perturbation with flooding is smaller than one without flooding and doesn’t cause the gradient vanishing or explosion like the losses without flooding after around 60,000 iterations.

However, from Figure 4, the losses fluctuation is so large that it is unclear whether applying flooding and the flood level affects the training at a moment. For example, it is

necessary to verify whether flooding is actually preventing the sharp drop in the discriminator’s loss, as represented in Figure 1. Therefore, we enlarged the images of the three cases (without flooding and with flooding (Medium, Over Opt)) in Figure 1 to verify the local fluctuations and provided the results at Figure 5.

Figure 5a shows the moment of gradient explosion and vanishing. It also demonstrates that the loss of the discriminator initially went down to nearly zero, and then the generator’s loss sharply dropped. This suggests that a sudden drop in the discriminator’s loss makes the training unstable. Whereas, as shown in Figure 5b, the discriminator’s loss is recovered with an appropriate flood level (Medium) when it drop suddenly. The result supports the claims made in the conceptual diagram of Figure 1.

However, if the flood level is too high (Over Opt), the loss before applying flooding moves below the flood level as Figure 5c. Occasionally, the loss of the discriminator increases and approaches the flood level, which means that the loss after applying flooding becomes lower, but then the loss decreases again. It needs further investigation to understand what the phenomenon implies.

To deepen the knowledge, we examined the relationship between flooding and the gradient of the generator and discriminator. We used the same experimental results, and calculated the L2 norm of gradients of the model’s final layers during GAN training.

Figure 6 shows the results. Overall, the gradient without flooding is larger than ones with flooding. It also supports that flooding prevents gradient vanishing or explosion and stabilizes GAN training.

E. Implementation of Section 4.5

When we used CDCGAN, we split the first convolution layer of DCGAN to two convolution layers for the input noise and the class label. After that, we concatenated output of the two convolution layers. We used the same layers as DCGAN for the second and the following layers, and gave the second layer the concatenated output as input.

Tzeng et al. define adversarial losses for ADDA,

$$\begin{aligned}
 L_{\text{adv}_D}(\mathbf{X}_s, \mathbf{X}_t, M_s, M_t) &= \mathbb{E}_{\mathbf{x}_s \sim \mathbf{X}_s} [f_{D,s}(D(M_s(\mathbf{x}_s)))] \\
 &\quad + \mathbb{E}_{\mathbf{x}_t \sim \mathbf{X}_t} [f_{D,t}(D(M_t(\mathbf{x}_t)))] \\
 &= \mathbb{E}_{\mathbf{x}_s \sim \mathbf{X}_s} [-\log(D(M_s(\mathbf{x}_s)))] \\
 &\quad + \mathbb{E}_{\mathbf{x}_t \sim \mathbf{X}_t} [-\log(1 - D(M_t(\mathbf{x}_t)))] ,
 \end{aligned} \tag{39}$$

where M_s and M_t are mappings from source domain \mathbf{X}_s and target domain \mathbf{X}_t to same representation space. We

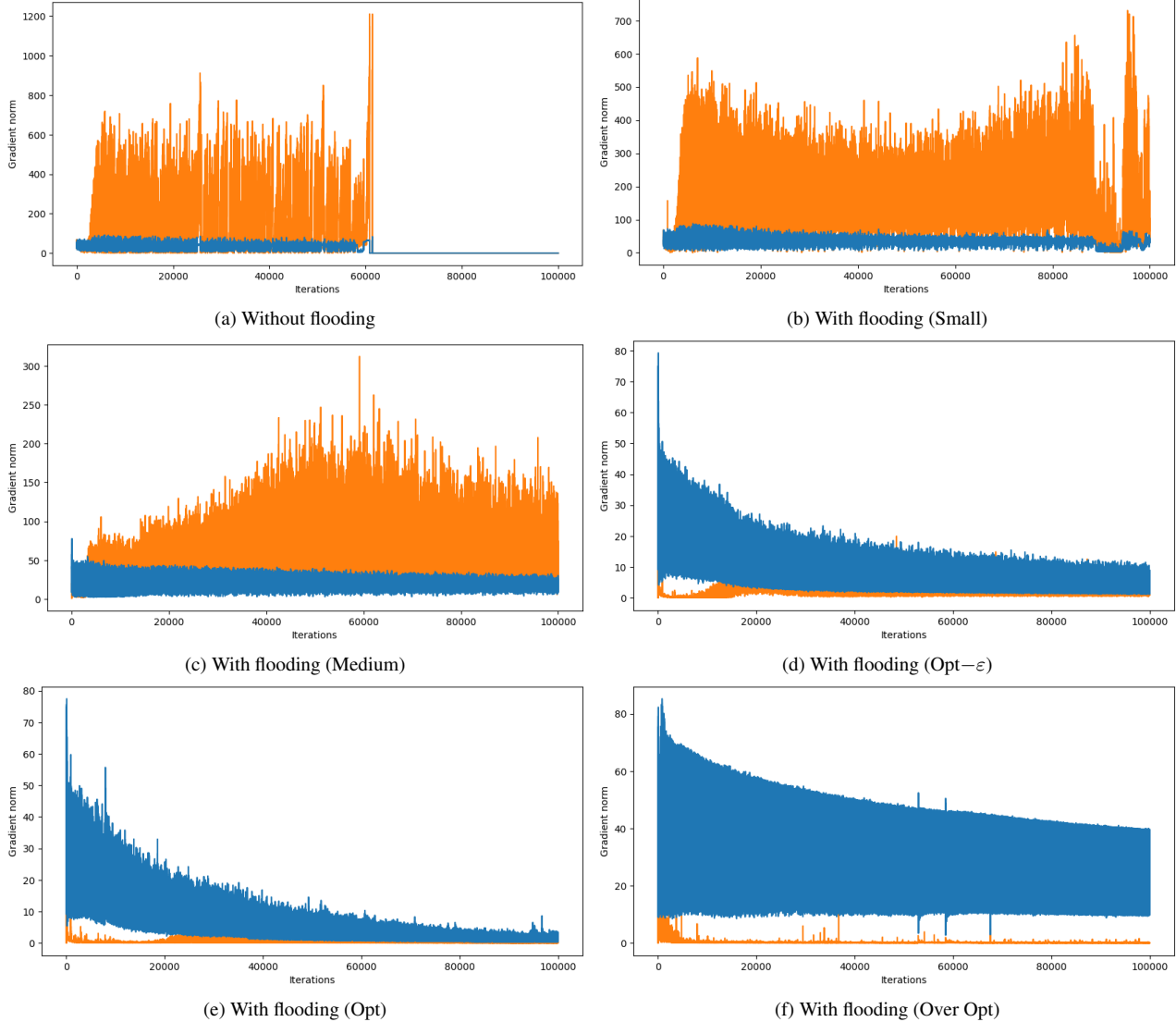


Figure 6. Transition of L2 norm of final layer’s gradient of the generator (orange) and discriminator (blue).

propose flooding for ADDA:

$$\begin{aligned}
 L_{\text{adv}_{D,\text{flood}}}(\mathbf{X}_s, \mathbf{X}_t, M_s, M_t) \\
 = h(\mathbb{E}_{\mathbf{x}_s \sim \mathbb{X}_s} [f_{D,s}(D(M_s(\mathbf{x}_s)))] \\
 + \mathbb{E}_{\mathbf{x}_t \sim \mathbb{X}_t} [f_{D,t}(D(M_t(\mathbf{x}_t)))] , b).
 \end{aligned}
 \tag{40}$$

We examined the flooding effects on $L_{\text{adv}_{D,\text{flood}}}$ with flood level b being $\log 2$. When we conducts experiments for ADDA, we adopted and modified the implementation described in Supplementary Section C.

Note that the experimental results for ADDA without flooding have deteriorated compared to the officially announced scores. However, given that no changes were made to the source code for the experiment without flooding, and there are questions about the reproducibility of other experiments in the issues, we determined that the score is not

an average but the best score. If we regard the results with flooding approach to the best score, it suggests that flooding enhances the stability of training in ADDA.